Applied Physics Letters

Realization of a nonlinear interferometer with parametric amplifiers

Cite as: Appl. Phys. Lett. **99**, 011110 (2011); https://doi.org/10.1063/1.3606549
Submitted: 27 February 2011 • Accepted: 11 June 2011 • Published Online: 08 July 2011

Jietai Jing, Cunjin Liu, Zhifan Zhou, et al.

APPLIED PHYSICS LETTERS 99, 011110 (2011)

Realization of a nonlinear interferometer with parametric amplifiers

Jietai Jing,[1] Cunjin Liu,[1] Zhifan Zhou,[1] Z. Y. Ou,[1,2,a)] and Weiping Zhang[1,b)]
[1]*Quantum Institute for Light and Atoms, Department of Physics, East China Normal University, Shanghai 200062, People's Republic of China*
[2]*Department of Physics, Indiana University-Purdue University Indianapolis, 402 N. Blackford Street, Indianapolis, Indiana 46202, USA*

(Received 27 February 2011; accepted 11 June 2011; published online 8 July 2011)

We construct an interferometer with parametric amplifiers as beam splitters. Because of the gain in the parametric amplifiers, the maximum output intensity of the interferometer can be much bigger than the input intensity as well as the intensity inside the interferometer (the phase sensing intensity). We find that the fringe intensity depends quadratically on the intensity of the phase sensing field at high gain. This type of nonlinear interferometer has better sensitivity than the traditional linear interferometer made of beam splitters with the same phase sensing intensity. © *2011 American Institute of Physics*. [doi:10.1063/1.3606549]

Optical interferometry is the basis for precision measurement. Traditional optical interferometer such as the Michelson interferometer played a pivotal role in the development of Einstein's special relativity.[1] Even at present day, it is still a central part of the design in Laser Interferometer Gravitational-Wave Observatory in search of the gravitational wave predicted by Einstein's general relativity.

A simple interferometer such as the Mach-Zehnder interferometer shown in Fig. 1(a) consists of two beam splitters with the one acting as wave splitter and the other as wave combiner. For simplicity of argument, we let them to be identical with a transmissivity T and reflectivity R. From any standard optics textbook,[2] we can find the output intensity is related to the input by

$$I_{out} = 2I_0TR(1+\cos\varphi) = I_F(1+\cos\varphi)/2, \qquad (1)$$

where I_0 is the input intensity and $I_F \equiv 4I_0TR$ is the maximum fringe intensity. The best sensitivity for measuring a small phase change occurs at $\varphi = \pi/2$ with

$$\Delta I_{out} = I_F\Delta\varphi/2 \equiv 2TI_{ps}\Delta\varphi, \qquad (2)$$

where $I_{ps} \equiv RI_0$ is the intensity of the field subject to a phase change (phase-sensing field). So, the sensitivity for phase measurement is directly related to the fringe intensity I_F and that for a linear interferometer is also proportional to the phase sensing intensity.

On the other hand, there are some nonlinear processes that are phase sensitive. Yurke *et al.* proposed in 1986 (Ref. 3) to use parametric processes to measure the phase and the sensitivity can reach the ultimate quantum limit of phase measurement, i.e., the Heisenberg limit.[4] There were numerous theoretical analyses on such a system, including a recent one by Plick *et al.* who suggested a further boost from a coherent state injection.[5] But there has been no experimental realization since its inception, perhaps because the output field in the original proposal by Yurke *et al.* is very weak to detect at experimentally controllable gain.

In this letter, we report on an experiment in which we construct a nonlinear interferometer with parametric amplifiers acting as beam splitters to split and recombine an incoming optical field. When properly balanced, the interferometer can in principle have 100% visibility. Since amplification is actively involved in the interferometer, the phase sensing field inside the interferometer is amplified from the input field and so is the output field exhibiting the interference fringe. Thus, the sensitivity can be greatly enhanced as compared to the traditional linear interferometer.

Consider the conceptual sketch in Fig. 1(b). Our interferometer consists of two parametric amplifiers (PA). The first PA (PA1) amplifies the input "signal" field and in the meantime produces a conjugate "idler" field. Thus, the first PA serves as a beam splitter and split the input field into two. The second PA (PA2) serves as a beam combiner, which mixes the amplified signal field and the idler field. The action of a parametric amplifier is well described in any nonlinear optics text book[6] as

$$A_s^{out} = GA_s^{in} + gA_i^{in*}; \quad A_i^{out} = GA_i^{in} + gA_s^{in*}. \qquad (3)$$

Here s and i stand for signal and idler, respectively. G is the amplitude gain of the amplifier and $|G|^2 - |g|^2 = 1$.

Therefore, if there is no idler field input at PA1, the fields after PA1 is

$$A_{s1} = G_1A_{s0}; \quad A_{i1} = g_1A_{s0}^*. \qquad (4)$$

Here, A_{s0} is the input signal field. Note that when the gain is large, $G_1 \approx g_1 \gg 1$ and we have a nearly equal splitting of A_{s0} but the split fields are amplified from the input. Assuming the idler field is subject to a phase shift of φ, we obtain the outputs of PA2 from Eqs. (3) and (4) as

$$A_{s2} = G(\varphi)A_{s0}; \quad A_{i2} = g(\varphi)A_{s0}^*, \qquad (5)$$

with

$$G(\varphi) = G_1G_2 + g_1^*g_2e^{-i\varphi}; \quad g(\varphi) = G_1^*g_2 + G_2g_1e^{i\varphi}. \qquad (6)$$

In the case when both amplifiers have the same gain: $G_1 = G_2 \equiv G_0$, $g_1 = g_2 = g_0$, we have (G_0, g_0 = real)

a)Electronic mail: zou@iupui.edu.
b)Electronic mail: wpzhang@phy.ecnu.edu.cn.

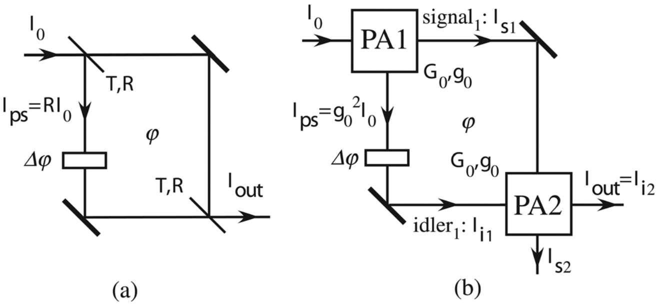

FIG. 1. (a) A linear Mach-Zehnder interferometer. (b) A nonlinear interferometer with parametric amplifiers (PA1 and PA2) as the equivalent beam splitters.

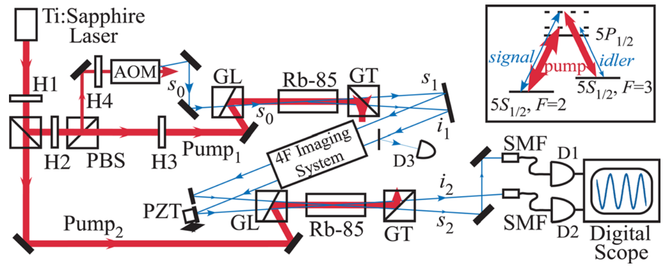

FIG. 2. (Color online) Layout for an experimental realization of the nonlinear interferometer. H: half wave plate; PBS: polarization beam splitter; AOM: acoustic optic modulator; GL: Glen laser polarizer; GT: Glen-Thompson polarizer; SMF: single-mode fiber; D: detector.

$$G(\varphi) = 1 + |g_0|^2(1 + e^{-i\varphi}); \quad g(\varphi) = G_0 g_0(1 + e^{i\varphi}). \tag{7}$$

From Eq. (4), we find the intensity of the phase sensing field (idler 1) inside the interferometer as

$$I_{i1} = |A_{i1}|^2 = |g_0|^2 I_0, \tag{8}$$

with $I_0 \equiv |A_{s0}|^2$ as the input intensity. The intensities of the output fields can also be easily obtained as

$$I_{s2} = I_0[1 + 2|G_0 g_0|^2(1 + \cos\varphi)], \quad I_{i2} = 2I_0|G_0 g_0|^2(1 + \cos\varphi). \tag{9}$$

So both the output fields show interference fringes when the phase is scanned. The idler side always has a visibility of 100%, but the signal side's visibility is

$$V_s = 2|G_0 g_0|^2/(1 + 2|G_0 g_0|^2), \tag{10}$$

which is close to 100% when $G_0, g_0 \gg 1$.

From Eq. (9), we find the maximum fringe intensity at the idler output to be

$$I_{i2}^M = 4I_0|G_0 g_0|^2 = 4|G_0|^2 I_{ps} = 4(I_{ps} + I_0)I_{ps}/I_0. \tag{11}$$

Here $I_{ps} \equiv I_{i1}$ is the intensity of the phase sensing field. For a large gain and a fixed input I_0, we have $I_{ps} \gg I_0$ and $I_{i2}^{(M)} \propto I_{ps}^2$. Eq. (11) is the main feature of this nonlinear interferometer that is different from a traditional linear interferometer, i.e., the maximum fringe intensity depends quadratically on the phase sensing intensity, in contrast to the linear dependence in Eq. (1) for a linear interferometer. Furthermore, the maximum fringe intensity is amplified from the phase sensing intensity by a factor of $4|G_0|^2$, giving an enhancement in sensitivity as compared to Eq. (2) for a linear interferometer.

The experimental layout is shown in Fig. 2. The two parametric amplifiers are based on a four-wave mixing process[7] of a lambda configuration in Rb-85 vapor cells (inset of Fig. 2). The two identical Rb vapor cells are 12 mm long and are temperature-stabilized at 117 °C. They are respectively illuminated by an intense vertically polarized pump beam (~400 mW) with a beam waist of 600 μm. The pump beams are from a frequency-stabilized Ti:Sapphire laser locked to a Fabry-Perot reference cavity. A horizontally polarized seed beam (usually known as "signal") with a beam waist of 350 μm is combined with the pump beam at an angle of 0.7° in the center of the first vapor cell by a Glan-laser polarizer. A Glan-Thompson polarizer at the output port of the vapor cell is used to filter out the pass-over residual pump beam. The pump laser frequency is about 0.8 GHz blue detuned from the Rb-85 $F = 2 \rightarrow F'$ transition at 795 nm and the seed signal beam is about 3.04 GHz red shifted from the pump with an acoustic optic modulator. Based on these settings, the seed signal beam is amplified by a gain, which depends on the power and frequency of the pump beam. In the meantime, a conjugate beam (usually dubbed "idler") with a frequency of 3.04 GHz blue shift from the pump is produced in the four-wave mixing process.

By using a 4f imaging system, we couple the outputs of the first vapor cell (the amplified signal and the conjugate idler beams) into the second vapor cell through another Glan-laser polarizer. They are symmetrically crossed with the pump at the center of the second vapor cell at 0.7°, similar to the first vapor cell. The two output beams from the

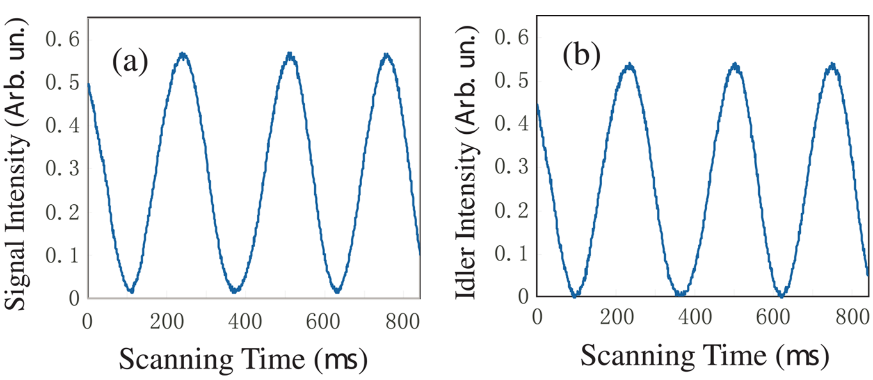

FIG. 3. (Color online) Interference fringes for the nonlinear interferometer. (a) Signal output. (b) Idler output.

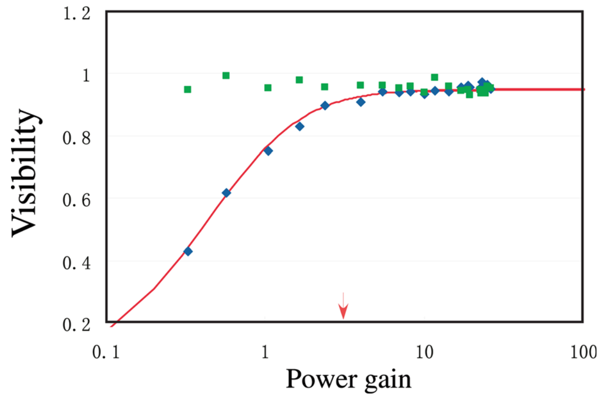

FIG. 4. (Color online) Visibility of interference fringe as a function of power gain $|g_0|^2$. Green squares: idler fringe; blue diamond: signal fringe; red solid line: plot of the function in Eq. (10); the function is multiplied by a factor of 0.95 for imperfect alignment. The arrow corresponds to the gain for Fig. 3.

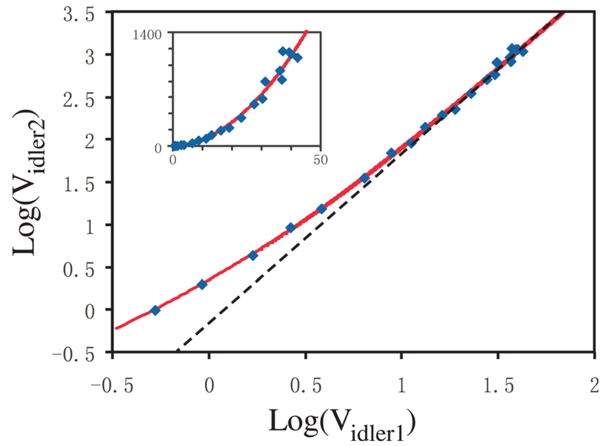

FIG. 5. (Color online) Logarithmic of the maximum intensity of the interference fringe as a function of logarithmic of the intensity of the phase sensing field inside the nonlinear interferometer. Inset: linear scale plot; red solid line: fit to the function in Eq. (11); dashed line: slope 2 for quadratic dependence.

second vapor cell are, respectively, sent to two photodiodes (D1 and D2) with single-mode fiber coupling for spatial mode clean up. The obtained photocurrents are fed to a digital scope for data collection and analysis. A mirror mounted on a piezo-electric transducer is used to change the phase of the signal and idler beams after the first cell for the phase scan of the interferometer. The relative power of the pump beams can be controlled by half wave plates H1, H2, and H3 while the power of the injected signal beam by H4.

Fig. 3 shows typical interference fringes at the two outputs of the interferometer. The relative power of the two pump beams to the two cells is optimized for maximum visibility ($P_1 = 420$ mW, $P_2 = 430$ mW). The signal output has a slightly smaller visibility (94.5%) than the idler side (98.6%), as expected from Eq. (10). Next, we measure the visibilities at different gains of the parametric amplifier by varying the power of the pump beams. Fig. 4 shows the results of the measurement. The red solid line is a plot of Eq. (10) multiplied by a factor of 0.95 to account for imperfect alignment of the interferometer. The visibility data of the signal fringe follow this line very well. Moreover, the visibility of the idler fringe is kept at constant around 95%, consistent with Eq. (9).

To confirm the nonlinear nature of the interferometer, we measure the maximum of the interference fringe of the idler output as a function of the intensity of the phase sensing field (the idler beam by D3 right after the first vapor cell) as we change the pump powers. The results are plotted in Fig. 5 in log-log scale. The solid red line is a best fit curve to Eq. (11) with I_0 as the adjustable parameter. The dashed black line is a straight line with a slope of two, showing the quadratic dependence. The inset is in linear scale clearly showing the nonlinear trend. Note that, at the highest value, the maximum fringe intensity is about 30 times the phase sensing intensity.

In conclusion, we demonstrate a nonlinear interferometer with a fringe intensity much higher than the equivalent linear interferometer, thus leading to an enhanced sensitivity for phase measurement. Although we did not discuss quantum noise performance of this nonlinear interferometer, it is shown elsewhere[8] to be also better than linear interferometers.

This work is supported by the National Natural Science Foundation of China under Grant Nos. 10828408, 10974057, and 10588402; the National Basic Research Program of China (973 Program) under Grant No. 2011CB921604; the Program of Shanghai Subject Chief Scientist under Grant No. 08XD14017; Shanghai Pujiang Program under Grant No.09PJ1404400; the program for Professor of Special Appointment (Eastern Scholar) at Shanghai Institutions of higher Learning; and the Program for New Century Excellent Talents in University.

[1]A. A. Michelson and E. W. Morley, Am. J. Sci. **34**, 333 (1887).
[2]M. Born and E. Wolf, *Principle of Optics* (Pergamon, Oxford, 1st ed., 1959; 7th ed., 1999).
[3]B. Yurke, S. L. McCall, and J. R. Klauder, Phys. Rev. A **33**, 4033 (1986).
[4]Z. Y. Ou, Phys. Rev. Lett. **77**, 2352 (1996).
[5]W. N. Plick, J. P. Dowling, and G. S. Agarwal, New J. Phys. **12**, 083014 (2010).
[6]R. Boyd, *Nonlinear Optics* (Academic, New York, 1992).
[7]C. F. McCormick, V. Boyer, E. Arimondo, and P. D. Lett, Opt. Lett. **32**, 178 (2007).
[8]Z. Y. Ou, "Enhancement of phase measurement sensitivity beyond standard quantum limit by a nonlinear interferometer" (to be published).